Journal Title
XX(X):1–9

Reprints and permission:
sagepub.co.uk/journalsPermissions.nav
DOI: 10.1177/ToBeAssigned
www.sagepub.com/

Kaimal spectrum based H2 optimization of tuned mass dampers for wind turbines

Somya Ranjan Patro[1], Arnab Banerjee[1], Sondipon Adhikari[2] and Gunturi Venkata Ramana[1]

Abstract

The closed form analytical expression of the objective function of a single degree of freedom system with tuned mass damper (TMD), subjected to Gaussian white noise and Kaimal forcing spectrum, is derived implementing the H_2 optimization technique. To illustrate the procedure, a wind turbine tower with and without TMD, subjected to wind load, has been presented. Kaimal spectrum has been considered to model the effects of wind load. Usually, the parameters of TMD is optimized by implementing H_2 optimization technique on Gaussian white noise (GWN) even though the system is subject to any other forcing spectrum. Obtaining an analytical closed form expression of the objective function for a TMD system considering a real spectrum is very challenging as a real spectrum may contains fractional order of the frequency. Therefore, either objective function can be obtained numerically or an analytical form can be obtained but only for GWN as an input forcing spectrum. To address the above mentioned issue, in this paper, the concept of near identity spectrum (NIS) is introduced to idealize the Kaimal spectrum with high accuracy from which a closed form expression of the objective function can be established. Further, histogram plots of the response reduction has been made to show a comparison between TMD system optimized with Gaussian white noise and Kaimal spectrum. The results showed that the displacement response of TMD system subjected to Kaimal spectrum yields better performance if it is optimized according to Kaimal spectrum rather than GWN and vice versa.

Keywords

Gaussian white noise; Kaimal Spectrum; Near Identity Spectrum; offshore wind turbine; H_2 Optimization

Introduction

A tuned mass damper (TMD) is a vibration control device which can be attached to a vibrating member (primary system) subjected to the dynamic forces or base excitation. A mass connected by a parallel spring and dashpot element with the primary system is the most common form of a TMD, was first proposed by (Ormondroyd 1928). The parameters of a TMD, i.e. spring stiffness and damping coefficient can be obtained by implementing two analytical optimization techniques, namely H_∞ and H_2 optimization.

The H_∞ optimization technique can be used to estimate the optimum parameters when the primary system is subjected to harmonic force/motion (Hahnkamm 1933; Brock 1946; Snowdon 1974; Warburton 1982). Minimization of the maximum amplitude magnification factor (called H_∞ norm) of the primary system is the key principle of the H_∞ optimization technique (Nishihara and Matsuhisa 1997; Ren 2001; Liu and Liu 2005; Wong and Cheung 2008; Cheung and Wong 2009). Den Hartog (1985) derived the optimum parameters of the TMD system based on the fixed-point theory for minimizing the maximum vibration velocity response of a single degree of freedom (SDOF) system under harmonic excitation. Anh and Nguyen (2014) proposed an approach to determine the approximate analytical solutions for the H_∞ optimization of the dynamic vibration absorber (DVA) attached to the damped primary structure subjected to force excitation by replacing with an equivalent undamped structure. A closed-form expression of the optimum parameters of a TMD can be obtained using the H_∞ optimization technique if and only if damping is not considered in the primary system (Ioi and Ikeda 1978; Randall et al. 1981; Thompson 1981; Soom and Lee 1983). For damped primary systems, several numerical and series solutions has been proposed for obtaining the optimum parameters as given in the state of the art (Sekiguchi and Asami 1984; Yamaguchi and Harnpornchai 1993; Tsai and Lin 1993; Asami et al. 1995; Zuo 2009). Liu and Coppola (2010) used numerical approaches namely Chebyshev's equioscillation theorem to study the optimum design of the damped primary system. Chun et al. (2015) studied the H_∞ optimal design of a DVA variant for suppressing high-amplitude vibrations of damped primary systems using diversity-guided cyclic-network-topology-based constrained particle swarm optimization (Div-CNTCPSO) technique. In contrary, the primary objective of the H_2 optimization technique is to reduce the total vibration energy of the system's overall frequency by minimizing the area under the frequency response curve (Warburton 1982; Asami et al. 1991, 2001). Several literature have proposed H_2

[1]Department of Civil Engineering, Indian Institute of Technology Delhi, India
[2]James Watt School of Engineering, The University of Glasgow, UK

Corresponding author:
Arnab Banerjee, Assistant Professor, Department of Civil Engineering, Indian Institute of Technology Delhi, Hauz Khas, New Delhi, 110016, India.
Email: abanerjee@civil.iitd.ac.in

optimization techniques to estimate the optimum parameters of TMD systems (Adhikari et al. 2016; Asami et al. 2002; Chowdhury et al. 2021; Adhikari and Banerjee 2021). Ghosh et al. (2007) obtained a closed form expression for optimum tuning ratio of damped TMD system subjected to harmonic load and GWN. Zuo (2009) conducted decentralized H_2 and H_∞ control methods to optimize the parameters of spring stiffness and damping coefficients for random and harmonic vibration. Cheung and Wong (2011) derived H_2 optimum parameters of a DVA to minimize the total vibration energy or the mean square motion of a single degree of freedom (SDOF) system under random force excitations. Chowdhury et al. (2022) compared the H_2 and H_∞ optimization methods to identify the optimal system parameters of different vibration control devices subjected to Gaussian white noise (GWN) and harmonic motion. All the studies mentioned above are conducted using GWN when the amplitude is constant over the frequency range . However, no one derived a closed-form expression of the objective function from which the optimum parameter of the TMD can be determined while the TMD is subjected to a forcing spectrum other than GWN.

Motivated from above-mentioned research gap, in the present study, a forcing spectrum is considered in which the amplitude is variable over the frequency domain which is more realistic in nature. As an example of a real spectrum, in this study, Kaimal spectrum is considered. Kaimal spectrum is often used to model the effect of wind load for offshore structures, tall buildings, cable stayed bridges, transmission towers etc. (Ankireddi and Y. Yang 1996; Commission et al. 2005; Det 2013; Tian and Gai 2015; Li et al. 2021). Since the function of the Kaimal spectrum usually contains fractional power of excitation frequency, the use of the H_2 optimization technique to estimate closed-form expression of the objective function can sometimes be arduous (Colwell and Basu 2009). To overcome the fractional power in the spectrum, a near identity spectrum (NIS) similar to the Kaimal spectrum is proposed in this paper, which helps in omitting the fractional power of excitation frequency. Finally, a closed-form expression can be obtained for the objective function after implementation of H_2 optimization technique. The time displacement responses have been compared between a traditional wind turbine and wind turbine attached with a TMD system. Finally, histogram plots have been made to show a comparison between the optimum parameters of the TMD system optimized for GWN and Kaimal spectrum.

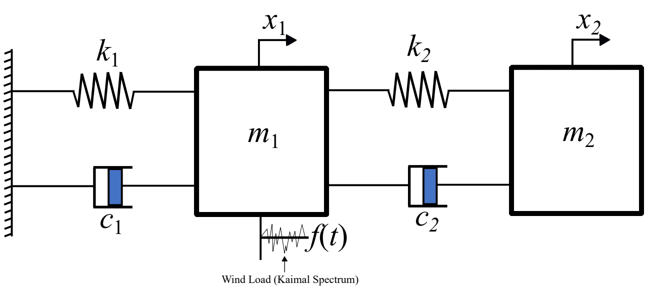

Figure 1. A tuned mass damper (TMD) system subjected to random wind load (Kaimal spectrum)

Methodology

Frequency Response Function

A single degree of freedom (SDOF) system equipped with a passive TMD is considered in the present study as shown in Figure 1. Since, the two degree of freedom system given in Figure 1 can be considered as the model given by (Asami et al. 2002) and defining several non-dimensional parameters such as mass ratio $\left(\mu = \frac{m_2}{m_1}\right)$, natural frequency of primary system $\left(\omega_1 = \sqrt{\frac{k_1}{m_1}}\right)$, primary system damping ratio $\left(\zeta_1 = \frac{c_1}{2m_1\omega_1}\right)$, natural frequency of TMD $\left(\omega_2 = \sqrt{\frac{k_2}{m_2}}\right)$, TMD damping ratio $\left(\zeta_2 = \frac{c_2}{2m_2\omega_2}\right)$, frequency ratio $\left(\nu = \frac{\omega_2}{\omega_1}\right)$ and non-dimensional excitation frequency $\left(\lambda = \frac{\omega}{\omega_1}\right)$ and substituting these parameters in the equation of motion of two degree of freedom system, Frequency Response Function (FRF) can be established as

$$H(\lambda) = \frac{\nu^2 + (i\lambda)^2 + 2\zeta_2\nu(i\lambda)}{\left(\begin{array}{l}(i\lambda)^4 + (2\zeta_1 + 2\nu\zeta_2 + 2\mu\nu\zeta_2)(i\lambda)^3 + \\ \left(1 + \nu^2 + \mu\nu^2 + 4\nu\zeta_1\zeta_2\right)(i\lambda)^2 + \\ \left(2\zeta_1\nu^2 + 2\zeta_2\nu\right)(i\lambda) + \nu^2\end{array}\right)} \tag{1}$$

Kaimal spectrum

Since, our two degree of freedom system is subjected to wind force which is considered as random load. Thus, following DNV code (Det 2013) the Kaimal spectrum (KS) is used to incorporate the effect of wind load. The theoretical KS for fixed point reference point in space can be written as

$$S_{uu,k}(\omega) = \frac{\sigma_U^2\left(\frac{4L_k}{\bar{U}}\right)}{\left(1 + \frac{3\omega L_k}{\pi\bar{U}}\right)^{\frac{5}{3}}} \tag{2}$$

where L_k is the integral length scale, $\bar{U}$ is the mean wind speed, σ_U is the standard deviation of mean wind speed and f is the excitation frequency in Hz. The spectral density of the turbulent thrust force on the rotor $S_{FF,wind,k}(\omega)$ following (Arany et al. 2015) can be written as

$$S_{FF,wind,k}(\omega) = \rho_a^2\frac{D^4\pi^2}{16}C_T^2\bar{U}^2\sigma_U^2\tilde{S}_{uu,k}(\omega) \tag{3}$$

where,

$$\tilde{S}_{uu,k}(\omega) = \frac{S_{uu,k}(\omega)}{\sigma_U^2} \tag{4}$$

and,

$$\sigma_U = I\bar{U} \tag{5}$$

where D is the diameter of the rotor, $\tilde{S}_{uu,k}(\omega)$ is the normalized Kaimal spectrum, ρ_a is the density of air, C_T is the thrust coefficient, I is the turbulence intensity. The thrust coefficient can be estimated using (Frohboese et al. 2010) as

$$C_T = \frac{7}{\bar{U}} \tag{6}$$

Since, angular excitation frequency ω is the only variable and all other parameters can be considered as a constant. Thus, equation (3) can be written as

$$S_{FF,k}\left(\omega\right)=\frac{\alpha}{\left(\beta\omega+1\right)^{\frac{5}{3}}} \tag{7}$$

Objective Function

Since, our TMD system is subjected to random load, to estimate the optimum parameters such as optimum frequency ratio (ν_{opt}) and TMD damping ratio (ζ_{2opt}), H_2 optimization technique (Asami et al. 2002) is used. In this method, standard deviation is considered as the objective function which is to be minimized. Thus, the standard deviation of displacement response can be derived following (Adhikari et al. 2016) as

$$\begin{aligned}\sigma_{xx}^2 &= E\left[x^2\left(t\right)\right]=R_{xx}\left(0\right)=\int_{-\infty}^{\infty}S_{FF}\left(\omega\right)\left|H\left(\omega\right)\right|^2 d\omega\\ &=\omega_1\int_{-\infty}^{\infty}S_{FF}\left(\lambda\right)\left|H\left(\lambda\right)\right|^2 d\lambda\end{aligned} \tag{8}$$

For simplification, equation (7) can be written in the form

$$S_{FF,k}\left(\lambda\right)=\frac{\alpha}{\left(\beta\omega+1\right)^{\frac{5}{3}}}=\frac{\alpha}{\left(\chi\lambda+1\right)^{\frac{5}{3}}} \tag{9}$$

where, $\chi=\beta\omega$ and $\omega=2\pi f$. Now, substituting equation (9) in equation (8), we obtain

$$\sigma_{xx}^2=\gamma\int_{-\infty}^{\infty}\frac{1}{\left(\chi\lambda+1\right)^{\frac{5}{3}}}\left|H\left(\lambda\right)\right|^2 d\lambda \tag{10}$$

where, $\gamma=\alpha\omega_1$

Validation for Gaussian White Noise (GWN)

When the TMD system is subjected to GWN, the Power Spectral Density (PSD) will be considered as constant wrt λ. Thus, equation (8) can be normalized as

$$I_{\min}=\frac{\sigma_{xx}^2}{2\pi\omega_1 S_{FF,k}}=\frac{1}{2\pi}\times\int_{-\infty}^{\infty}\left|H\left(\lambda\right)\right|^2 d\lambda \tag{11}$$

where, I_{min} is the performance index which is a non-dimensional form of variance. Now, to evaluate the integration of equation (11), (Newland 1993) suggested a methodology in which the integrand must be in the form of

$$H\left(\lambda\right)=\frac{B_0+\left(i\lambda\right)B_1+\left(i\lambda\right)^2B_2+\cdots\left(i\lambda\right)^{n-1}B_{n-1}}{A_0+\left(i\lambda\right)A_1+\left(i\lambda\right)^2A_2+\cdots\left(i\lambda\right)^{n}A_{n}} \tag{12}$$

Since, equation (1) is a 4^{th} order polynomial of λ, substituting $n=4$ in equation (12) we obtain

$$H\left(\lambda\right)=\frac{B_0+i\lambda B_1-\lambda^2B_2-i\lambda^3B_3}{A_0+i\lambda A_1-\lambda^2A_2-i\lambda^3A_3+\lambda^4A_4} \tag{13}$$

Now, comparing equation (1) and equation (13) we obtain the coefficients as

$$\begin{aligned}&B_0=\nu^2, B_1=2\zeta_2\nu, B_2=1, B_3=0\\ &A_1=2\zeta_1\nu^2+2\zeta_2\nu\\ &A_2=1+\nu^2+\mu\nu^2+4\nu\zeta_1\zeta_2\\ &A_3=2\zeta_1+2\nu\zeta_2+2\mu\nu\zeta_2\\ &A_4=1\end{aligned} \tag{14}$$

$$I_{\min}=\frac{\left\{\begin{array}{l}A_0B_3^2\left(A_0A_3-A_1A_2\right)\\ +A_0A_1A_4\left(2B_1B_3-B_2^2\right)\\ -A_0A_3A_4\left(B_1^2-2B_0B_2\right)\\ +A_4B_0^2\left(A_1A_4-A_2A_3\right)\end{array}\right\}}{2A_0A_4\left(A_0A_3^2+A_4A_1^2-A_1A_2A_3\right)} \tag{15}$$

Figure 2 shows the contour of Performance Index I_{min} for different frequency ratio (ν) and TMD damping ratio (ζ_2). From Figure 2, it can be observed that when a TMD is subjected to GWN having mass ratio ($\mu=0.1$) and primary system damping ratio ($\zeta_1=0.01$), the optimum frequency ratio (ν_{opt}) was found to be 0.93 and the optimum TMD damping ratio (ζ_{2opt}) was found to be 0.15. equation (15) is also validated with (Asami et al. 2002) for different values of mass ratio μ and primary system damping ratio ζ_1 as shown in Figure 3.

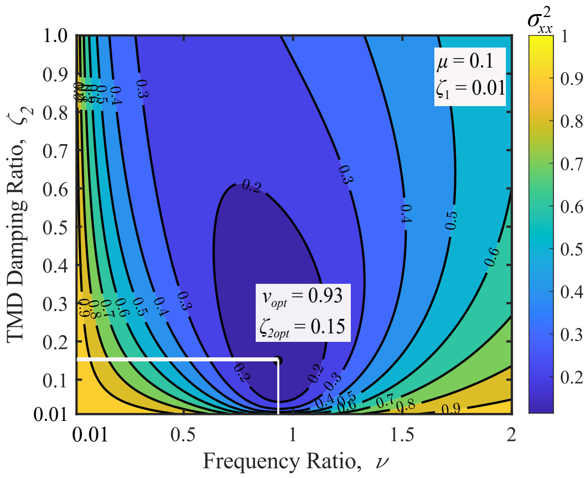

Figure 2. Contour of Performance Index I_{min} for different frequency ratio (ν) and TMD damping ratio (ζ_2) subjected to Gaussian white noise

Optimization for Kaimal Spectrum

For TMD system subjected to Kaimal Spectrum, a closed form equation of the objective function given in equation (8) cannot be directly obtained due to presence of fractional power of λ in the integrand. Thus, solving it numerically, a contour plot has been made for different frequency ratio (ν) and TMD damping ratio (ζ_1) as shown in Figure 4. From Figure 4, it can be observed that when a TMD is subjected to Kaimal Spectrum having mass ratio ($\mu=0.1$), primary system damping ratio ($\zeta_1=0.01$) and a non-dimensional parameter ($\chi=100$), the optimum frequency ratio (ν_{opt}) was found to be 0.91 and the optimum TMD damping ratio (ζ_{2opt}) was found to be 0.15. The non-dimensional parameter ($\chi=100$) mainly depends on mean wind velocity

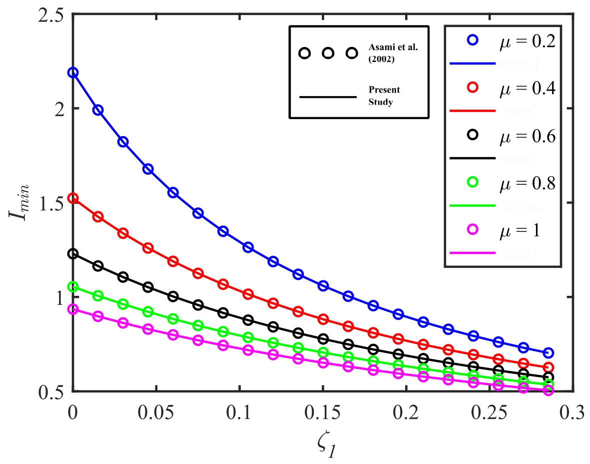

Figure 3. Validation with (Asami et al. 2002) for different values of mass ratio μ and primary system damping ratio ζ_1

$\bar{U}$, integral length scale L_k and natural frequency of the primary system (ω_1) and it has been observed that, higher value of χ does not have a much effect in the change of optimum parameters but, for lesser of χ, the value of optimum frequency ratio (ν_{opt}) tends toward optimum frequency ratio (ν_{opt}) of Gaussian white noise.

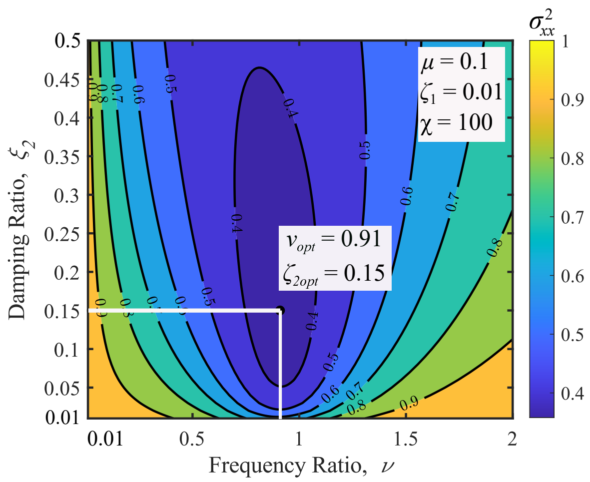

Figure 4. Contour of Variance σ^2_{xx} for different frequency ratio (ν) and TMD damping ratio (ζ_2) subjected to Kaimal spectrum. Here, the integral of equation (10) has been solved numerically to obtain the contour plot.

Near Identity Spectrum

Now, to estimate the objective function for TMD system subjected to Kaimal spectrum analytically, a near identity spectrum (NIS) has been established such that the power spectral density function can be written as

$$\begin{aligned} S_{FF,k}(\lambda) &= \frac{\alpha}{(\chi\lambda+1)^{\frac{5}{3}}} \\ \approx S_{FF,n}(\lambda) &= \frac{\alpha\delta\left(1+\varepsilon^2\lambda^2\right)}{(1+\chi^2\lambda^2)(1+\phi^2\lambda^2)} \end{aligned} \tag{16}$$

where, δ, ε and ϕ are constants which depends on χ. Now, using non-linear regression technique and curve fitting method, a relationship can be developed between δ, ε and ϕ as a function of χ. The relationships can be expressed as

$$\delta = p_1\chi^3 + p_2\chi^2 + p_3\chi + p_4 \tag{17}$$

$$\varepsilon = q_1 \ln(\chi) + \frac{q_2}{\chi^2} + \frac{q_3}{\chi} + q_4\chi + q_5 \tag{18}$$

and,

$$\phi = r_1 e^{(-r_2\chi)} + r_3\chi^2 + r_4\chi + r_5 \tag{19}$$

where, $p_1 = 4.685 \times 10^{-8}$, $p_2 = -4.897 \times 10^{-5}$, $p_3 = 0.02069$, $p_4 = 0.9586$, $q_1 = -0.1308$, $q_2 = 1.307$, $q_3 = -2.748$, $q_4 = 0.0003$, $q_5 = 1.74$, $r_1 = -0.6364$, $r_2 = 0.2823$, $r_3 = 1.82 \times 10^{-7}$, $r_4 = -0.0001584$ and $r_5 = 0.6684$. Now, comparing equation (16) for Kaimal spectrum and Near Identity Spectrum in Figure 5, we can observe that the Near Identity Spectrum almost coincides with the Kaimal spectrum and can be used as a substitute of Kaimal spectrum for further calculations. Now, to conduct H_2 optimization, substituting equation (16) in equation (8) and modifying equation (8) as

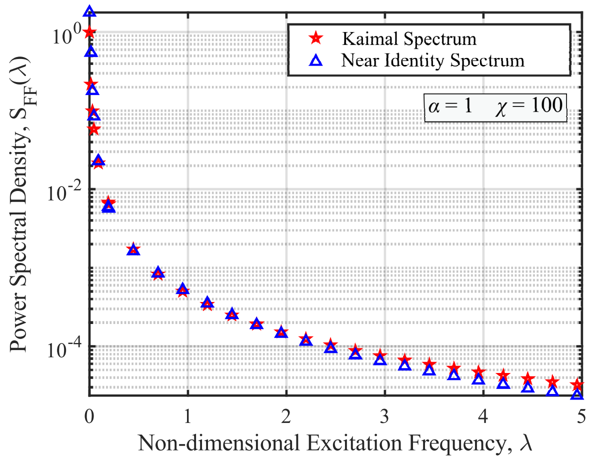

Figure 5. Comparison between Kaimal spectrum and Near Identity spectrum (NIS)

$$\sigma_x^2 = \alpha\omega_1\delta \int_{-\infty}^{\infty} |T(\lambda)|^2 d\lambda = \frac{\pi\alpha\omega_1 M_6}{a_0\Delta_6} \tag{20}$$

where, the values of $T(\lambda)$, M_6 and Δ_6 including the entire derivation of the integral in equation (20) is given in annex section. Figure 6 shows a contour of Variance (σ_x^2) for different frequency ratio (ν) and TMD damping ratio (ζ_1). From Figure 6, it can be observed that when a TMD is subjected to NIS having mass ratio ($\mu = 0.1$), primary system damping ratio ($\zeta_1 = 0.01$) and non-dimensional parameter ($\chi = 100$), the optimum frequency ratio (ν_{opt}) was found to be 0.91 and the optimum TMD damping ratio (ζ_{2opt}) was found to be 0.15 which exactly matches with the optimum parameters of Figure 4 which provides us essential confidence to use the NIS as a substitution spectrum of Kaimal spectrum.

Results and Discussions

Time Domain Response

Using the concept of inverse fast Fourier transform, time domain wind force can be represented as sum of N sinusoids

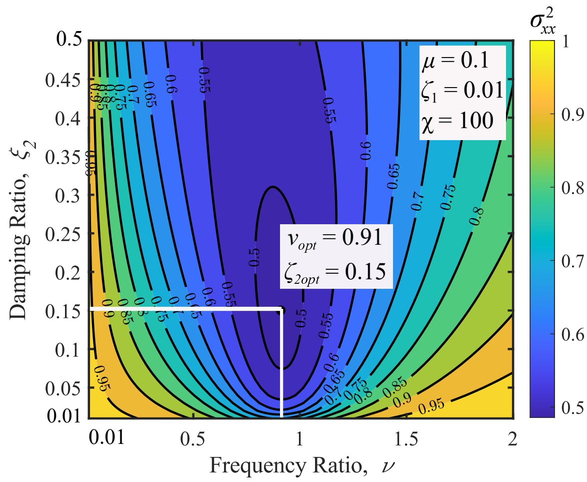

Figure 6. Contour of Variance σ^2_{xx} for different frequency ratio (ν) and TMD damping ratio (ζ_2) for the Near Identity Spectrum (NIS). Here, the integral of equation (20) has been solved analytically to obtain the contour plot.

of amplitude A_i at an angular frequency ω_i having phase angle φ_i:

$$F_{wind} = \sum_{i=1}^{N} A_i \sin(\omega_i t + \varphi_i) \quad (21)$$

the amplitude can be determined from the power spectral density of turbulent thrust force as

$$A = \sqrt{2S_{FF}(f)} \quad (22)$$

Now, using MATLAB tool called ode solver and assuming the initial conditions for displacement and velocity as zero, the time domain response can be evaluated. Considering a example model of Siemens SWT-107-3.6 offshore wind turbine (Arany et al. 2015) and using the method given by (Adhikari and Bhattacharya 2011) where the entire wind turbine system can be converted into a SDOF system, the time displacement response curve has been calculated for SDOF system, TMD optimised for GWN and TMD optimised for NIS subjected to GWN as shown in Figure 7 (a to d). Similarly, all the three cases were subjected to Wind Load and the response was shown in Figure 8 (a to d). In both Figure 7 and Figure 8, a sample size of 10k was considered and mean and standard deviation were plotted both for individual cases shown in Figure 7 (a to c) and Figure 8 (a to c) as well as a comparison has also been done considering all the cases as shown in Figure 7 (d) and Figure 8 (d). The wind turbine properties and the wind load properties are given in Table 1. A damping ratio (ζ_1) of 0.01 is also been considered for the wind turbine model.

Histogram plots

Although, a clear understanding is formed i.e., TMD system shows a significant reduction in displacement than conventional SDOF system irrespective of loading condition, but a clear comparison between the TMD GWN and TMD NIS is difficult to obtain from Figure 7 (d) and Figure 8 (d). Thus, to omit the confusion, histogram plots has been made for the response reduction between TMD optimised through GWN and TMD optimised through NIS subjected to GWN and Kaimal spectrum considering the same sample size of 10k as shown in Figure 9(a and b). Here, the response reduction can be defined as

$$RR\,(\%) = \frac{y_{normKS} - y_{normGWN}}{y_{normKS}} \times 100 \quad (23)$$

where, $y_{normGWN} = L_2$ norm or root mean square of the displacement responses of the TMD system optimized by Gaussian white noise and $y_{normKS} = L_2$ norm or root mean square of the displacement responses of the TMD system optimized by Kaimal Spectrum. When the TMD is subjected to Gaussian white noise, then the histogram of response reduction is more inclined towards positive side in other words positive area is more than negative area as shown in Figure 9 (a) whereas when the TMD system is subjected to Kaimal Spectrum, then the response reduction is more inclined towards negative side or more negative area as shown in Figure 9 (b). This clearly indicates, if the system is subjected to Gaussian white noise, then displacement response will be minimum when optimized according to GWN. Similarly, if the system is subjected to kaimal spectrum, then displacement response will be minimum when optimized according to kaimal spectrum.

Table 1. Wind Turbine and wind load properties for Siemens SWT-107-3.6 offshore wind turbine (Arany et al. 2015).

Property	Symbols	Values
Diameter of rotor (m)	D	107
Density of air (kg/m^3)	ρ_a	1.225
Mean wind speed (m/s)	U	9
Turbulence intensity	I	0.1
Integral length scale	L_k	340.2
Drag Coefficient	C_D	0.5
Young's modulus of the tower material (GPa)	E	210
Tower height (m)	L	5.0
Bottom Diameter (m)	D_b	5.0
Top Diameter (m)	D_t	3.0
Tower wall thickness (mm)	t	50
Tower mass (kg)	M_t	260000
Rotor nacelle assembly (RNA) mass (kg)	M_{RNA}	234500
Lateral foundation stiffness (GNm^{-1})	K_L	3.65
Rotational foundation stiffness (GNmrad^{-1})	K_R	254.3

Conclusion

A classical mechanics-based methodology towards the estimation of optimum parameters of a tuned mass damper (TMD) system subjected to Kaimal Spectrum using H_2 optimization technique has been communicated in this paper. The optimal parameters of a TMD is obtained by minimizing the the standard deviation of the displacement response, known as H_2 optimization technique. A validation study has been conducted with the existing literature for the TMD system subjected to Gaussian white noise (GWN). Since, obtaining an analytical closed form expression of the objective function for a TMD system considering a real spectrum, having fractional order of the frequency, is very challenging. Therefore, usually objective functions

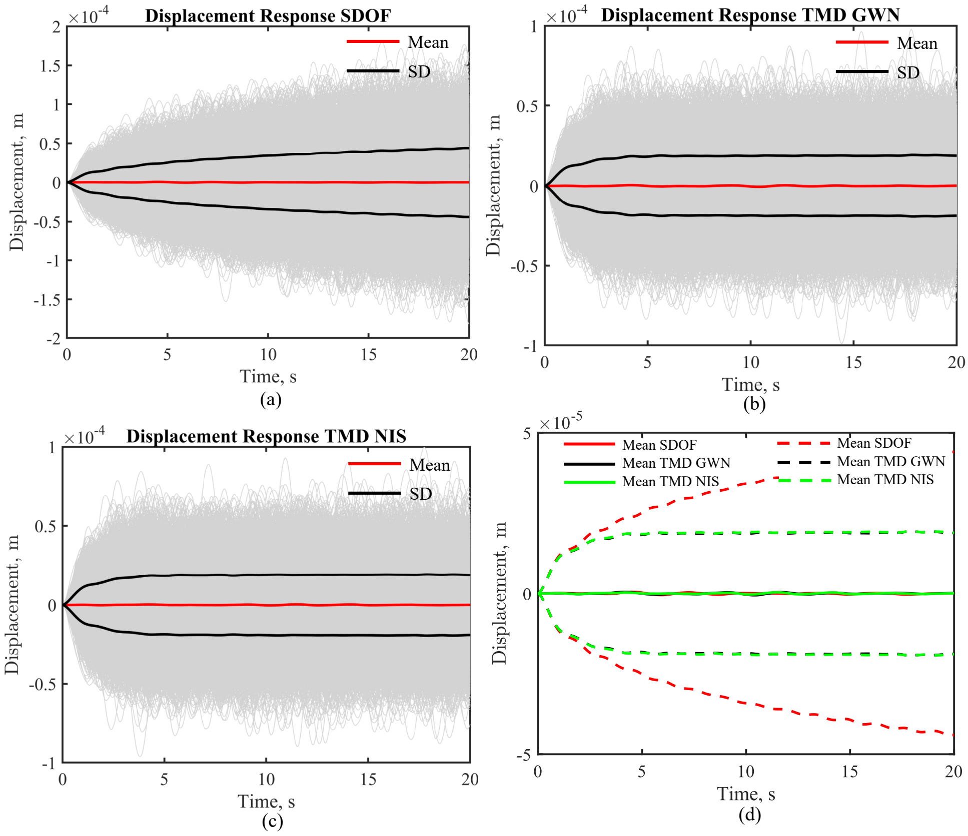

Figure 7. (a), (b) and (c) Time displacement curve including mean and standard deviation for SDOF, TMD optimised for GWN and TMD optimised for NIS subjected to GWN; (d) Mean and standard deviation comparison between all the three cases subjected to GWN

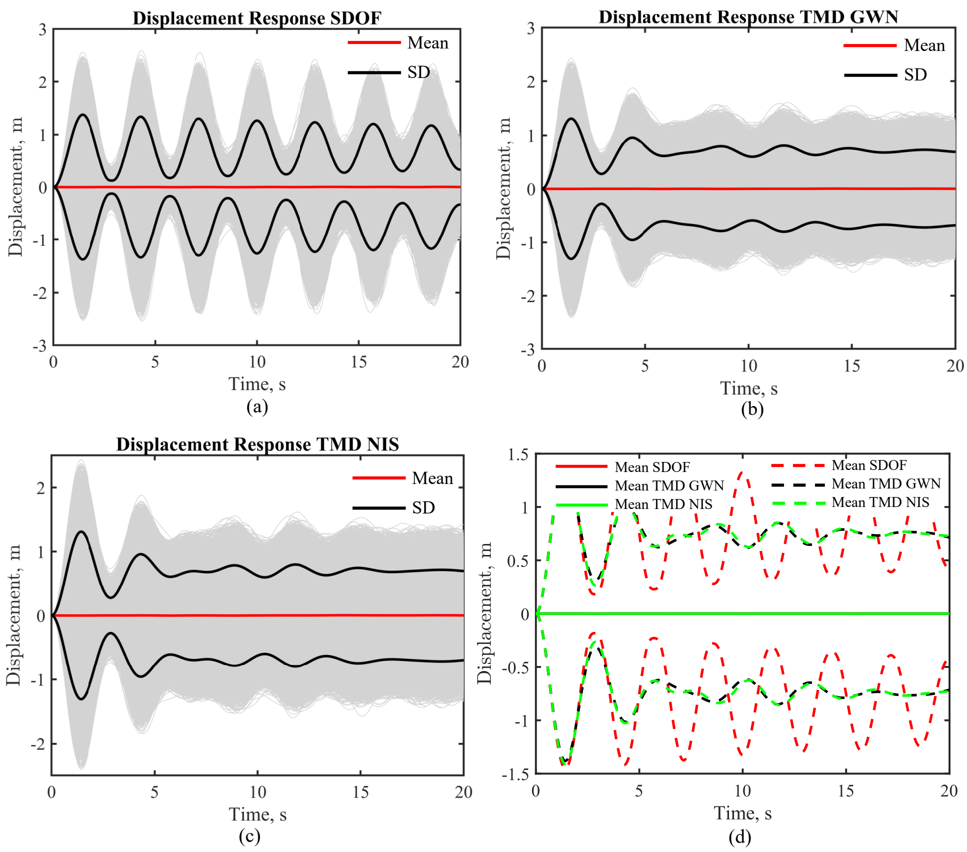

Figure 8. (a), (b) and (c) Time displacement curve including mean and standard deviation for SDOF, TMD optimised for GWN and TMD optimised for NIS subjected to KS; (d) Mean and standard deviation comparison between all the three cases subjected to KS

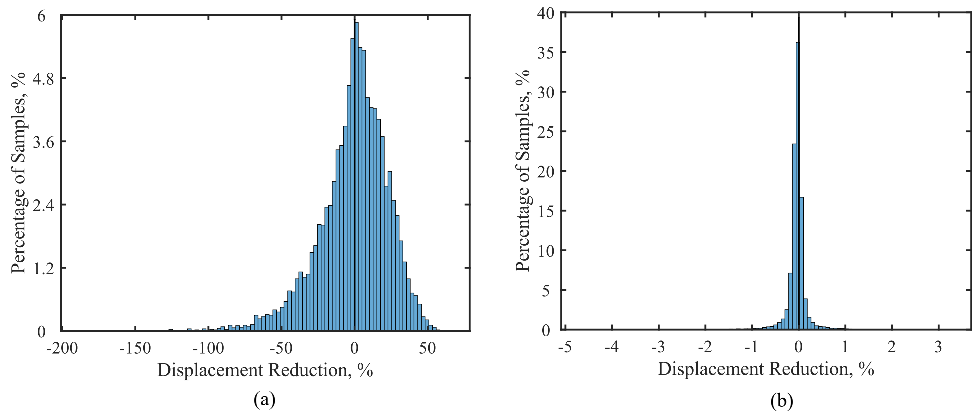

Figure 9. (a) and (b) Histogram plot for performance reduction when the system subjected to GWN and KS

are obtained numerically which does not directly yields the optimum point and increases the computational cost significantly. To deal with the aforementioned challenges associated with the fractional power of excitation frequency in the power spectral density, a concept of near identity spectrum (NIS) has been proposed. The NIS contains excitation frequency as a product of complex conjugate which enables us to form a closed-form expression of the objective function. The proposed NIS precisely matches with the Kaimal Spectrum; hence, it omits the fractional power in the variance equation. The closed-form analytical expression of objective function can be directly plotted to obtain the optimal parameters of the TMD system. A sample of ten thousand time histories obtained from GWN and Kaimal spectrum are applied to the system as in input force to realize the performance of the optimized TMD. From the histogram plot it can be concluded that, minimum displacement response occurs while the system be optimized according to the input forcing spectrum rather than any other noise/spectrum. Thus, the novelty lies in proposing a NIS that can be used as a generalized spectrum to estimate the optimum parameters of the TMD system implementing the H_2 optimization technique. Due to severe change in climatic condition in recent years, the demand of stable, clean and green energy production becomes the primary mission of several countries. Towards this mission, the developed NIS contributed for easy simulation of wind load and provides a generalised method for optimal design which can be used in design firms for next generation wind turbine design and control. Further, this concept of NIS could be extended in the future study to generalize other dynamic loads, such as wave loads, earthquake loads, etc.

Annexure

The values of $T(\lambda)$, M_6, Δ_6 and derivation of the integral in equation (20) are listed below.

$$T(\lambda) = \frac{B_0(i\lambda)^3 + B_1(i\lambda)^2 + B_2(i\lambda) + B_3}{\begin{pmatrix} A_0(i\lambda)^6 + A_1(i\lambda)^5 + A_2(i\lambda)^4 \\ +A_3(i\lambda)^3 + A_4(i\lambda)^2 + A_5(i\lambda) \\ +A_6 \end{pmatrix}}, \tag{24}$$

in which,

$$B_0 = \varepsilon, \tag{25}$$

$$B_1 = 2\nu\varepsilon\zeta_2 + 1, \tag{26}$$

$$B_2 = \varepsilon\nu^2 + 2\zeta_2\nu, \tag{27}$$

$$B_3 = \nu^2, \tag{28}$$

$$A_0 = \chi\phi, \tag{29}$$

$$A_1 = \chi + \phi + 2\chi\phi\zeta_1 + 2\chi\nu\phi\zeta_2 + 2\chi\mu\nu\phi\zeta_2, \tag{30}$$

$$A_2 = \begin{pmatrix} \chi\phi + 2\chi\zeta_1 + 2\phi\zeta_1 + \chi\nu^2\phi + 2\chi\nu\zeta_2 \\ +2\nu\phi\zeta_2 + 2\chi\mu\nu\zeta_2 + 2\mu\nu\phi\zeta_2 + \chi\mu\nu^2 v \\ +4\chi\nu\phi\zeta_1\zeta_2 + 1 \end{pmatrix}, \tag{31}$$

$$A_3 = \begin{pmatrix} \chi + \phi + 2\zeta_1 + 2\nu\zeta_2 + \chi\nu^2 + \\ \nu^2\phi + \mu\nu^2\phi + 2\mu\nu\zeta_2 + \chi\mu\nu^2 + \\ 2\chi\nu\phi\zeta_2 + 4\chi\nu\zeta_1\zeta_2 + 4\nu\phi\zeta_1\zeta_2 + 2\chi\nu^2\phi\zeta_1 \end{pmatrix}, \tag{32}$$

$$A_4 = \begin{pmatrix} \mu\nu^2 + \nu^2 + \chi\nu^2\phi + 2\chi\nu^2\zeta_1 + 2\nu^2\phi\zeta_1 \\ +2\chi\nu\zeta_2 + 2\nu\phi\zeta_2 + 4\nu\zeta_1\zeta_2 + 1 \end{pmatrix}, \tag{33}$$

$$A_5 = 2\nu\zeta_2 + \chi\nu^2 + \nu^2\phi + 2\nu^2\zeta_1 \tag{34}$$

and,

$$A_6 = \nu^2 \tag{35}$$

To evaluate equation (20), (James et al. 1947) suggested a method in which the integrand must be in the form of

$$I_n = \frac{1}{2\pi j}\int_{-\infty}^{\infty} \frac{g_n(x)}{h_n(x)\,h_n(-x)}dx \tag{36}$$

where,

$$g_n(x) = b_0 x^{2n-2} + b_1 x^{2n-4} + \cdots + b_{n-1} \tag{37}$$

and,

$$h_n(x) = a_0 x^n + a_1 x^{n-1} + \cdots + a_n \tag{38}$$

Now, by assuming $q = i\lambda$ and writing integrand of Eq.(20) in form of integrand of Eq.(36) as

$$\frac{g_6(x)}{h_6(x)\,h_6(-x)} = \frac{\begin{pmatrix} C_0x^6 + C_1x^4 + \\ C_2x^2 + C_3 \end{pmatrix}}{\left\{ \begin{pmatrix} A_0x^6 + A_1x^5 + A_2x^4 \\ +A_3x^3 + A_4x^2 + A_5x \\ +A_6 \end{pmatrix} \begin{pmatrix} A_0x^6 - A_1x^5 + A_2x^4 \\ -A_3x^3 + A_4x^2 - A_5x \\ +A_6 \end{pmatrix} \right\}} \tag{39}$$

where,

$$C_0 = -u^2 \tag{40}$$

$$C_1 = (2\nu u\zeta_2 + 1)^2 - 2u\left(u\nu^2 + 2\zeta_2\nu\right) \tag{41}$$

$$C_2 = 2\,(2\nu u\zeta_2 + 1)\,\nu^2 - \left(u\nu^2 + 2\zeta_2\nu\right)^2 \tag{42}$$

and,

$$C_3 = \nu^4 \tag{43}$$

Since, the highest power of x in Eq.(39) is 6, thus, substituting $n = 6$ in Eq.(36), Eq.(37) and Eq.(38), we obtain the integrand as

$$\frac{g_6(x)}{h_6(x)\,h_6(-x)} = \frac{\begin{pmatrix} b_0x^{10} + b_1x^8 + b_2x^6 + b_3x^4 \\ +b_4x^2 + b_5 \end{pmatrix}}{\left\{ \begin{pmatrix} a_0x^6 + a_1x^5 + a_2x^4 + \\ a_3x^3 + a_4x^2 + a_5x + a_6 \end{pmatrix} \begin{pmatrix} a_0x^6 - a_1x^5 + a_2x^4 - \\ a_3x^3 + a_4x^2 - a_5x + a_6 \end{pmatrix} \right\}} \tag{44}$$

Now, comparing Eq.(39) and Eq.(44) we obtain the coefficients as $b_0 = b_1 = 0$, $b_2 = C_0$, $b_3 = C_1$, $b_4 = C_2$, $b_5 = C_3$ and $a_i = A_i$ where, $i = 1$ to 6. Thus, Eq.(20) can be evaluated as

$$\sigma_{xx}^2 = 2\pi\alpha\omega_1 \times \frac{1}{2\pi j} \int_{-\infty}^{\infty} \frac{g_6(x)}{h_6(x)\,h_6(-x)} dx = \frac{\pi\alpha\omega_1 M_6}{a_0 \Delta_6} \tag{45}$$

where,

$$M_6 = \begin{pmatrix} b_0d_0 + a_0b_1d_1 + a_0b_2d_2 + \\ a_0b_3d_3 + a_0b_4d_4 + \frac{a_0b_5}{a_6} d_5 \end{pmatrix} \tag{46}$$

and,

$$\Delta_6 = \begin{pmatrix} a_0^2a_5^3 + 3a_0a_1a_3a_5a_6 - 2a_0a_1a_4a_5^2 - \\ a_0a_2a_3a_5^2 - a_0a_3^3a_6 + a_0a_3^2a_4a_5 + a_1^3a_6^2 - \\ 2a_1^2a_2a_5a_6 - a_1^2a_3a_4a_6 + a_1^2a_4^2a_5 + a_1a_2^2a_5^2 + \\ a_1a_2a_3^2a_6 - a_1a_2a_3a_4a_5 \end{pmatrix} \tag{47}$$

where,

$$d_0 = \begin{pmatrix} -a_0a_3a_5a_6 + a_0a_4a_5^2 - a_1^2a_6^2 + 2a_1a_2a_5a_6 \\ +a_1a_3a_4a_6 - a_1a_4^2a_5 - a_2^2a_5^2 - a_2a_3^2a_6 \\ +a_2a_3a_4a_5 \end{pmatrix}, \tag{48}$$

$$d_1 = -a_1a_5a_6 + a_2a_5^2 + a_3^2a_6 - a_3a_4a_5, \tag{49}$$

$$d_2 = -a_0a_5^2 - a_1a_3a_6 + a_1a_4a_5, \tag{50}$$

$$d_3 = a_0a_3a_5 + a_1^2a_6 - a_1a_2a_5, \tag{51}$$

$$d_4 = a_0a_1a_5 - a_0a_3^2 - a_1^2a_4 + a_1a_2a_3 \tag{52}$$

and,

$$d_5 = \begin{pmatrix} a_0^2a_5^2 + a_0a_1a_3a_6 - 2a_0a_1a_4a_5 \\ -a_0a_2a_3a_5 + a_0a_3^2a_4 - a_1^2a_2a_6 + a_1^2a_4^2 \\ +a_1a_2^2a_5 - a_1a_2a_3a_4 \end{pmatrix} \tag{53}$$

References

Adhikari S and Banerjee A (2021) Enhanced low-frequency vibration energy harvesting with inertial amplifiers. *Journal of Intelligent Material Systems and Structures* : 1045389X211032281.

Adhikari S and Bhattacharya S (2011) Vibrations of wind-turbines considering soil-structure interaction. *Wind and Structures* 14(2): 85.

Adhikari S, Friswell M, Litak G and Khodaparast HH (2016) Design and analysis of vibration energy harvesters based on peak response statistics. *Smart Materials and Structures* 25(6): 065009.

Anh N and Nguyen NX (2014) Design of non-traditional dynamic vibration absorber for damped linear structures. *Proceedings of the Institution of Mechanical Engineers, Part C: Journal of Mechanical Engineering Science* 228(1): 45–55.

Ankireddi S and Y Yang HT (1996) Simple atmd control methodology for tall buildings subject to wind loads. *Journal of Structural Engineering* 122(1): 83–91.

Arany L, Bhattacharya S, Macdonald J and Hogan SJ (2015) Simplified critical mudline bending moment spectra of offshore wind turbine support structures. *Wind Energy* 18(12): 2171–2197.

Asami T, Hosokawa Y et al. (1995) Approximate expression for design of optimal dynamic absorbers attached to damped linear systems (2nd report, optimization process based on the fixed-points theory). *Transactions of the Japan Society of Mechanical Engineers, Series C* 61(583): 915–922.

Asami T, Nishihara O and Baz AM (2002) Analytical solutions to h_∞ and h_2 optimization of dynamic vibration absorbers attached to damped linear systems. *J. Vib. Acoust.* 124(2): 284–295.

Asami T, Nishihara O, Baz AM and Kimura F (2001) Closed-form exact solution to h2 optimization of dynamic vibration absorbers attached to damped linear systems. *Trans Jpn Soc Mech Eng* 67(655): 597–603.

Asami T, Wakasono T, Kameoka K, Hasegawa M and Sekiguchi H (1991) Optimum design of dynamic absorbers for a system subjected to random excitation. *JSME international journal. Ser. 3, Vibration, control engineering, engineering for industry* 34(2): 218–226.

Brock JE (1946) A note on the damped vibration absorber. *Journal of Applied Mechanics* .

Cheung Y and Wong W (2009) Design of a non-traditional dynamic vibration absorber. *The Journal of the Acoustical Society of America* 126(2): 564–567.

Cheung Y and Wong WO (2011) h_2 optimization of a non-traditional dynamic vibration absorber for vibration control of structures under random force excitation. *journal of sound and vibration* 330(6): 1039–1044.

Chowdhury S, Banerjee A and Adhikari S (2021) Enhanced seismic base isolation using inertial amplifiers. In: *Structures*, volume 33. Elsevier, pp. 1340–1353.

Chowdhury, S, Banerjee, A and Adhikari, S (2022) Optimal negative stiffness inertial-amplifier-base-isolators: Exact closed-form expressions. In: *International Journal of Mechanical Sciences*. Elsevier, pp. 107044.

Chun S, Lee Y and Kim TH (2015) h_∞ optimization of dynamic vibration absorber variant for vibration control of damped linear systems. *journal of sound and vibration* 335: 55–65.

Colwell, S., and Basu, B. (2009) Tuned liquid column dampers in offshore wind turbines for structural control *Engineering structures* 31: 358–368.

Commission IE et al. (2005) Iec 61400-1: Wind turbines–part 1: Design requirements.

Den Hartog JP (1985) *Mechanical vibrations*. Courier Corporation.

Det N (2013) Dnv offshore standard dnv-os-j101, design of offshore wind turbine. *Technical Standard* : 134–135.

Frohboese P, Schmuck C and Hassan GG (2010) Thrust coefficients used for estimation of wake effects for fatigue load calculation. In: *European Wind Energy Conference*. pp. 1–10.

Ghosh, Aparna and Basu, Biswajit (2007) A closed-form optimal tuning criterion for TMD in damped structures. In: *Structural Control and Health Monitoring* 14(4): pp. 681–692.

Hahnkamm E (1933) Die dämpfung von fundamentschwingungen bei veränderlicher erregerfrequenz. *Ingenieur-Archiv* 4(2): 192–201.

Ioi T and Ikeda K (1978) On the dynamic vibration damped absorber of the vibration system. *Bulletin of JSME* 21(151): 64–71.

James HM, Nichols NB and Phillips RS (1947) *Theory of servomechanisms*, volume 25. McGraw-Hill New York.

Li Y, Zhu L, Qian C, Jian X and Sun L (2021) The time-varying modal information of a cable-stayed bridge: Some consideration for shm. *Engineering Structures* 235: 111835.

Liu K and Coppola G (2010) Optimal design of damped dynamic vibration absorber for damped primary systems. *Transactions of the Canadian Society for Mechanical Engineering* 34(1): 119–135.

Liu K and Liu J (2005) The damped dynamic vibration absorbers: revisited and new result. *Journal of sound and vibration* 284(3-5): 1181–1189.

Newland D (1993) An introduction to random vibrations, spectral and wavelet analysis. *Essex, England: Longman Scientific & Technical* .

Nishihara O and Matsuhisa H (1997) Design and tuning of vibration control devices via stability criterion. *Preparation of the Japan Society of Mechanical Engineering* 97: 165–168.

Ormondroyd J (1928) The theory of the dynamic vibration absorber. *Trans., ASME, Applied Mechanics* 50: 9–22.

Randall S, Halsted III D and Taylor D (1981) Optimum vibration absorbers for linear damped systems. *Journal of Mechanical Design* .

Ren M (2001) A variant design of the dynamic vibration absorber. *Journal of sound and vibration* 245(4): 762–770.

Sekiguchi H and Asami T (1984) Theory of vibration isolation of a system with two degrees of freedom: 1st report, motion excitation. *Bulletin of JSME* 27(234): 2839–2846.

Snowdon J (1974) Dynamic vibration absorbers that have increased effectiveness. *Journal of Manufacturing Science and Engineering* .

Soom A and Lee Ms (1983) Optimal design of linear and nonlinear vibration absorbers for damped systems. *Journal of Vibration and Acoustics* .

Thompson A (1981) Optimum tuning and damping of a dynamic vibration absorber applied to a force excited and damped primary system. *Journal of Sound and Vibration* 77(3): 403–415.

Tian L and Gai X (2015) Wind-induced vibration control of power transmission tower using pounding tuned mass damper. *Journal of Vibroengineering* 17(7): 3693–3701.

Tsai HC and Lin GC (1993) Optimum tuned-mass dampers for minimizing steady-state response of support-excited and damped systems. *Earthquake engineering & structural dynamics* 22(11): 957–973.

Warburton G (1982) Optimum absorber parameters for various combinations of response and excitation parameters. *Earthquake Engineering & Structural Dynamics* 10(3): 381–401.

Wong WO and Cheung Y (2008) Optimal design of a damped dynamic vibration absorber for vibration control of structure excited by ground motion. *Engineering Structures* 30(1): 282–286.

Yamaguchi H and Harnpornchai N (1993) Fundamental characteristics of multiple tuned mass dampers for suppressing harmonically forced oscillations. *Earthquake engineering & structural dynamics* 22(1): 51–62.

Zuo L (2009) Effective and robust vibration control using series multiple tuned-mass dampers. *Journal of Vibration and Acoustics* 131(3).